HNUE JOURNAL OF SCIENCE
Natural Science, 2025, Volume 70, Issue 3, pp. 47-57
This paper is available online at http://hnuejs.edu.vn/ns
DOI: 10.18173/2354-1059.2025-0036

SELF-DIFFUSION OF BCC INTERSTITIAL ALLOY FeSi

Nguyen Quang Hoc[1], Pham Duy Thanh[2] and Duong Dai Phuong[3,*]
[1]*Faculty of Physics, Hanoi National University of Education, Hanoi city, Vietnam*
[2]*Faculty of Physics, Hanoi Pedagogical University 2, Phu Tho province, Vietnam*
[3]*Faculty of Fundamental Sciences, Military College of Tank Armor Officer, Phu Tho province, Vietnam*
*Corresponding author: Duong Dai Phuong, e-mail: tsphuong79@gmail.com

Received July 9, 2025. Revised September 13, 2025. Accepted September 30, 2025.

Abstract. In this work, we present analytical formulations for self-diffusion parameters, namely the activation energy, pre-exponential factor, and self-diffusion coefficient as functions of temperature, pressure, interstitial atom concentration, and strain in a BCC interstitial binary alloy, derived using the statistical moment method (SMM). These theoretical models are utilized to perform numerical simulations for the FeSi alloy. The computed SMM values for FeSi are compared with those obtained for pure Fe. The SMM results for Fe show strong consistency with existing experimental measurements and alternative computational data. The additional SMM findings are novel and offer predictions that can guide future experimental investigations.
Keywords: FeSi, self-diffusion, activation energy, pre-exponential factor, self-diffusion coefficient.

1. Introduction

Interstitial alloys, as well as metallic alloys in general, are widely utilized in materials science and engineering, and have become a focus of significant research interest. One of the major challenges in materials science and solid-state physics is understanding how atoms diffuse within crystalline solids [1]-[6]. A more comprehensive insight into atomic diffusion can be achieved by analyzing how stress influences diffusion behavior [7], [8]. The statistical moment method (SMM) is a powerful tool that can be used to investigate a wide range of properties, including structural, thermodynamic, elastic, diffusion, and phase transitions. It applies to various crystalline systems, including metals, alloys, semiconductor compounds, nanostructured materials, ionic and molecular crystals, inert and quantum gases, thin films, and two-dimensional materials like graphene. These studies span multiple lattice types, such as BCC, FCC, HCP,

and diamond structures across broad temperature ranges, from absolute zero to the melting point, and under varying pressure conditions [9]-[20]. In interstitial alloys, the primary constituent is a metal, typically present at concentrations of 90% or higher. This component is referred to as the main (or fundamental) metal. Interstitial alloys also contain additional elements, often non-metals, which are added in small quantities to impart specific properties [21]. These minor components occupy the spaces between metal atoms rather than replacing them. Such alloys are usually stabilized by chemical bonding. An interstitial alloy can be regarded as a solid solution, where the smaller non-metallic atoms occupy the interstitial sites of the metallic crystal lattice. The elements commonly found as interstitial atoms include H, B, C, N, O, and Si. The crystal structure of the alloy is dictated by the structure of the primary metal.

In binary interstitial systems, the host metal remains at the lattice points, while interstitial elements usually at low concentrations and with small atomic radii such as Si, Li, H, etc. occupy interstitial sites [21]. Typical Fe-based interstitial alloys, including FeSi, FeC, FeH, and FeS, are widespread due to their relevance to the Earth's core composition and industrial applications [22]. Among them, FeC is extensively used, accounting for over 80% of Fe alloy production, primarily because of its mechanical strength and durability. This has drawn significant attention to FeC from researchers. For instance, Takeuchi (1969) [23] examined the elastic behavior of FeC and showed that C content could reach up to 2.3%. More recently, studies by Melnykov and Davidchack (2018) [24] used MD simulations to explore the melting process of FeC, while Lau et al. (2007) [25] employed many-body techniques to model its behavior. Additional thermodynamic and elastic investigations using modified atomistic models were carried out by Liyanageet al. (2014) [26], and high-pressure studies up to 100 GPa were conducted by Nguyen et al. (2020) [27].

Beyond carbon, other light elements such as hydrogen can also enter the Fe lattice. Hydrogen has recently gained considerable attention, particularly in FeH systems under pressure. Studies like those of Ppin et al. (2014) [28] and Terasaki et al. (2012) [29] have explored FeH as a possible model for understanding the Earths inner core. Psiachos et al. (2011) [30] investigated Fe-H systems using *ab initio* methods and found that the H concentration could rise to around 11.1%. Their findings indicated a direct relationship between hydrogen content and changes in elastic constants, suggesting that hydrogen significantly influences FeHs mechanical properties. Lee and Jang (2007) [31] also highlighted the importance of incorporating hydrogen into atomistic modeling through the modified embedded atom method (MEAM).

Silicon as an interstitial element in Fe lattices has similarly attracted attention. Shibazaki et al. (2016) [22] demonstrated that the sound velocity in FeSi is not only structure-dependent but also influenced by Si content at pressures up to 6.3 GPa and temperatures of 800 K. Odkhuu et al. (2012) [32] studied the alloys resistivity and magnetic behavior, highlighting its potential in developing energy-efficient devices using density functional theory. There have been many theoretical studies on ternary alloys,

such as the investigation of FeCrSi using *ab initio* combined with DFT and GGA by Zhang et al. (2020) [33], in which the Si concentration affects the thermal expansion coefficient and Youngs modulus. Equilibrium thermal vacancy concentrations have been experimentally studied in $\mathrm{Fe_3Si}$ alloys [34]. The electronic and thermodynamic properties of B2-FeSi can also be investigated by *ab initio* methods, in which the full-potential plane-wave method (FPPW) is combined with the quasi-harmonic Debye (QHD) model (Zhao et al., 2011 [35]). Guo et al. (2000) [36] used CALPHAD modeling to examine how the melting points of TaSi and WSi change with Si concentration at ambient pressure. Additionally, Hoc et al. (2021) [37] used SMM to analyze the melting behavior, volume changes, enthalpy, and entropy of WSi with BCC structural defects under high pressure.

In this study, we present analytical formulations for self-diffusion parameters, including activation energy, pre-exponential factors, and diffusion coefficients, as functions of variables such as temperature, applied pressure, interstitial atom concentration, and strain, within BCC-type binary interstitial alloys. These theoretical models are developed using the SMM framework and are specifically applied to the FeSi alloy through detailed numerical simulations.

2. Content

The equilibrium concentration of vacancies in a defective alloy AB can be expressed as

$$n_\nu = \exp\left(-\frac{g_\nu^f(AB)}{k_{\mathrm{B}}T}\right) = n_\nu^A \exp\left(-\frac{c_B g_\nu^f(B)}{k_{\mathrm{B}}T}\right) \exp\left(-\frac{\sum_{X=A_1,A_2,A_3} c_X g_\nu^f(X)}{k_{\mathrm{B}}T}\right). \tag{2.1}$$

Here, the contribution from the interstitial atom B is disregarded due to its very low concentration. For a body-centered cubic (BCC) structure, the relations, $c_A = 1 - 7c_B$, $c_{A_1} = 2c_B$ and $c_{A_2} = 4c_B$ hold. In this expression, k_{B} is the Boltzmann constant, and $g_\nu^f(X)$ represents the variation in the Gibbs free energy of atom X associated with vacancy formation.

The change in Gibbs free energy for vacancy formation of atom X is given by

$$g_\nu^f(X) = -u_{0X} + \Delta\psi_X + P\Delta V_X, \tag{2.2}$$

where $\Delta\psi_X$ denotes the Helmholtz free energy change when an atom X is displaced from its lattice site to form a vacancy, u_{0X} is the cohesive energy, and ΔV_X is the volume variation due to the formation of a vacancy.

At zero pressure and temperature T, the activation energy of the crystal is defined as

$$Q_X(0,T) = -u_{0X}(0,T) + \Delta\psi_X(0,T) - \Delta_X^{(1)}(0,T), \tag{2.3}$$

where $\Delta\psi_X = (B_X - 1)\psi_X$, and $\Delta_X^{(1)} = (B_X^{(1)} - 1)\psi_X^{(1)}$ is the Helmholtz free energy change of atom X in the first coordination sphere surrounding the vacancy. The terms B_X and $B_X^{(1)}$ are dimensionless parameters related to energy ratios, approximated as

$$B_X \approx 1 + \frac{u_{0X}}{\psi_X},\ B_X^{(1)} \approx 1 + \frac{u_{0X} - \Delta\psi_X}{2\psi_X^{(1)}}. \tag{2.4}$$

The pre-exponential factor of the crystal at zero pressure and temperature T is given by

$$D_{0X}(0,T) = \frac{n_1 f \omega_X r_{1X}^2}{2\pi} \exp\left(\frac{s_\nu^f(X)}{k_\mathrm{B}}\right), \tag{2.5}$$

in which n_1 denotes the number of atoms located in the first coordination shell, f is the correlation factor, ω_X is the vibration frequency of the diffusing atom X, and r_{1X} refers to the effective jump distance. The term $s_\nu^f(X)$ represents the entropy related to the formation of a vacancy, which is approximated by considering the first and second nearest neighbor shells around the vacancy site, with their respective atom counts being n_1 and n_2,

$$s_\nu^f(X) = \frac{1}{n_1 + n_2}\Bigg[\frac{\partial u_{0X}}{\partial T} - (B_X - 1)\frac{\partial \psi_X}{\partial T} - \frac{g_\nu^f(X) + \dfrac{\partial u_{0X}}{\partial T} - (B_X - 1)\dfrac{\partial \psi_X}{\partial T}}{k_\mathrm{B}T^2} g_\nu^f(X) + k_\mathrm{B}\ln(N+1)\Bigg]. \tag{2.6}$$

The self-diffusion coefficient of the crystal at zero pressure and temperature T is then given by

$$D_X(0,T) \approx D_{0X}(0,T)\exp\left(-\frac{Q_X(0,T)}{k_\mathrm{B}T}\right). \tag{2.7}$$

In addition, the activation volume for atom X is defined as

$$V^a(X) = V^f(X) + V^m(X) = \nu(X) + V^r(X) + V^m(X), \tag{2.8}$$

where $\nu(X) = V^f(X) - V^r(X)$ is the difference between the vacancy formation volume $V^f(X)$ and the lattice recovery volume $V^r(X) = N\dfrac{4}{\sqrt{3}}\left(a_{AB}^{R3} - a_{AB}^3\right)$, with a_{AB} and a_{AB}^R are the mean atomic distances between two atoms of type A in the perfect and defective alloys, respectively, N denotes the number of atoms in the unit cell, and $V^m(X)$ is the migration volume associated with vacancy movement (Aziz, 1997 [19]).

The influence of strain on the pre-exponential factor of a crystal at zero pressure can be expressed as

$$D_X(\varepsilon) = D_{0X}(0,T)\exp\left(\frac{\sigma_0 \varepsilon^\alpha \left[V^r(X) + V^m(X)\right]}{k_\mathrm{B}T}\right), \tag{2.9}$$

where $\sigma = \sigma_0 \varepsilon^\alpha$ represents the applied stress, with σ_0 and α being material-specific parameters, and ε is the applied strain.

The dependence of the self-diffusion coefficient on strain at zero pressure is given by

$$D_X(\varepsilon) = D_{0X}(\varepsilon) \exp\left(-\frac{Q_X(0,T)}{k_\mathrm{B}T}\right). \tag{2.10}$$

The pressure dependence of the pre-exponential factor of the crystal is given by

$$D_{0X}(P) = D_{0X}(0,T) \exp\left(-\frac{PV^a(X)}{k_\mathrm{B}T}\right). \tag{2.11}$$

Similarly, the self-diffusion coefficient under pressure is given by

$$D_X(P) = D_{0X}(0,T) \exp\left(-\frac{Q_X(0,T)}{k_\mathrm{B}T}\right). \tag{2.12}$$

If the concentration of interstitial atom B is negligible (i.e., $c_\mathrm{B} = 0$), then the strain and pressure dependence of the diffusion coefficient for alloy AB reduces to that of the base metal A.

In this study, the self-diffusion theory outlined above is applied to the binary alloy FeSi. To model the atomic interactions within this alloy, the Mie–Lennard–Jones pair potential is employed. The interactions between Fe–Fe, Si–Si, and Fe–Si atom pairs are approximated using the following expression

$$\varphi(r) = \frac{D}{n-m}\left[m\left(\frac{r_0}{r}\right)^n - n\left(\frac{r_0}{r}\right)^m\right], \tag{2.13}$$

and the interaction potential for Fe–Si is approximated by

$$\varphi_{\mathrm{Fe-Si}} \approx \frac{1}{2}\left(\varphi_{\mathrm{Fe-Fe}} + \varphi_{\mathrm{Si-Si}}\right). \tag{2.14}$$

In these equations, D represents the depth of the potential well, while r_0 is the equilibrium separation between atoms. The parameters m and n are empirical exponents, determined through fitting to experimental data. The values of these parameters are listed in Table 1.

The effects of temperature, pressure, chemical composition, and mechanical strain on the diffusion characteristics of Fe and FeSi are systematically presented in Tables 2 through 6 and further illustrated in the accompanying figure.

Table 2 presents the calculated values of the pre-exponential factor D_0, the activation energy Q, and the self-diffusion coefficient D for Fe under the conditions $P = 0$ and $T = 1000$ K, using the statistical moment method (SMM).

Table 1. Parameters of the potential Mie–Lennard–Jones for interactions Fe–Fe and Si–Si [40], [41]

Interaction	m	n	D (10^{-16} erg)	r_0 (10^{-10} m)
Fe–Fe	7.0	11.5	6416.448	2.4775
Si–Si	6.0	12.0	45128	2.295

Table 2. The pre-exponential factor D_0, activation energy Q and self-diffusion coefficient D of Fe at $P = 0$, $T = 1000$ K calculated by SMM

Method	**Metal**	D_0 (cm^2/s)	Q (kcal/mol)	D (cm^2/s)
SMM	Fe	0.026	56.80	8.707×10^{-17}

The effects of temperature and silicon concentration on the activation energy Q and diffusion coefficient D, as calculated using the Statistical Moment Method (SMM) for Fe and FeSi, are presented in Table 3.

Table 3. $Q(T, c_{\mathrm{Si}})$ and $D(T, c_{\mathrm{Si}})$ for Fe, FeSi at $P = 0$ calculated by SMM

T (K)	$c_{\mathrm{Si}} = 0$		$c_{\mathrm{Si}} = 1\%$		$c_{\mathrm{Si}} = 3\%$	
	Q (kcal/mol)	$10^{20}D$ (cm^2/s)	Q (kcal/mol)	$10^{24}D$ (cm^2/s)	Q (kcal/mol)	$10^{33}D$ (cm^2/s)
700	25.17	0.02167	28.43	0.01710	35.80	0.02208
750	32.13	0.04891	35.91	0.08048	44.37	0.5163
800	38.25	0.5625	42.46	1.761	51.82	45.97
850	43.67	3.710	48.24	20.48	58.35	1845
900	48.51	43.23	53.38	432.3	64.11	432.3×10^2
950	52.86	432.3	57.98	4323	69.23	432.3×10^4

As indicated in Table 3, interstitial Si atoms significantly influence diffusion behavior in the FeSi alloy. For example, at a temperature of 1000K, when the Si concentration increases from 0% to 3%, the activation energy Q rises from 56.80 to 73.80 kcal/mol, which corresponds to a 29.93% increase. In FeSi, both the activation energy and the self-diffusion coefficient D exhibit an increasing trend with temperature. Notably, the diffusion rate escalates substantially as the temperature rises. When the temperature increases from 700 K to 1000 K, the change in activation energy per temperature unit $\Delta Q/\Delta T$ is estimated to be $0.105/(\mathrm{mol.K})$ for Fe, $0.127/(\mathrm{mol.K})$ for FeSi containing 1% Si, and approximately $5.66 \times 10^{-4}/(\mathrm{mol.K})$ for FeSi containing 3% Si. The rate of change in diffusion coefficient with respect to temperature is $\Delta D/\Delta T = 2.902 \times 10^{-19}$ cm^2/(s $\cdot$ K) for pure Fe. For FeSi containing 1% and 3% Si, the corresponding values are around 6.264×10^{-20} cm^2/(s$\cdot$K) and 1.092×10^{-27} cm^2/(s$\cdot$K),

respectively, as determined using the SMM.

When the concentration of Si in FeSi increases, the diffusion coefficient decreases sharply. Specifically, at 1000 K, increasing the Si concentration from 0% to 3% results in a reduction of the diffusion coefficient by as much as 99.99%. In general, diffusion in metals is only appreciable at elevated temperatures; at lower temperatures, it is negligible. This indicates that significant atomic migration in metallic systems primarily occurs under high thermal conditions.

Consequently, introducing Si atoms into interstitial sites within the Fe lattice reduces the diffusion coefficient D and raises the activation energy Q. This is due to enhanced atomic packing that limits the available space for atomic movement, thereby restricting atomic mobility and making it more challenging for atoms to migrate and form vacancies.

Table 4. Ratio $\dfrac{V^a}{\nu}(c_{\mathrm{Si}})$ ***as a function of silicon concentration in FeSi near its melting point, calculated by SMM***

$\boldsymbol{c_{\mathrm{Si}} = 0}$	$\boldsymbol{c_{\mathrm{Si}} = 1\%}$	$\boldsymbol{c_{\mathrm{Si}} = 2\%}$
0.89	0.91	0.94

Table 4 outlines the variation of the volume ratio with silicon content in FeSi, where V^a represents the vacancy activation volume and ν denotes the difference between this activation volume and the lattice recovery volume.

Meanwhile, Table 5 presents the diffusion coefficient D of FeSi as a function of strain ε, temperature, and Si concentration, calculated using SMM. The results indicate that D decreases as ε (or tensile stress) increases. This trend aligns well with the behavior observed in pure Fe.

Table 5. $\boldsymbol{D(T, \varepsilon, c_{\mathrm{Si}})}$ $(\mathrm{cm}^2/\mathrm{s})$ ***for FeSi calculated by SMM***

$\boldsymbol{c_{\mathrm{Si}}}$ $(\%)$	$\boldsymbol{T}$ **(K)**	$\boldsymbol{\varepsilon = 1\%}$	$\boldsymbol{\varepsilon = 3\%}$	$\boldsymbol{\varepsilon = 5\%}$
0	700	2.061×10^{-22}	1.853×10^{-22}	1.641×10^{-22}
	850	3.525×10^{-20}	3.158×10^{-20}	2.782×10^{-20}
	1000	8.264×10^{-17}	7.370×10^{-17}	6.462×10^{-17}
1	700	1.625×10^{-26}	1.458×10^{-26}	1.288×10^{-26}
	850	1.945×10^{-23}	1.739×10^{-23}	1.526×10^{-23}
	1000	1.775×10^{-19}	1.582×10^{-19}	1.367×10^{-19}
3	700	2.094×10^{-35}	1.872×10^{-35}	1.642×10^{-35}
	850	1.748×10^{-30}	1.457×10^{-30}	1.354×10^{-30}
	1000	3.101×10^{-25}	2.753×10^{-25}	2.359×10^{-25}

The dependence of $\ln D$ on $1000/T$ and the concentration of Si for FeSi at P = 0 GPa is illustrated in Figure 1. The plot in Figure 1 is linear and shows that the diffusion coefficient obeys the Arrhenius law of diffusion.

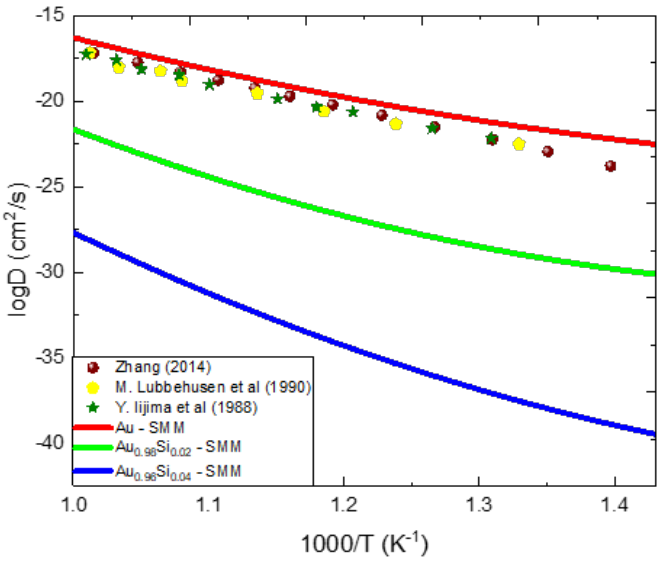

Figure 1. Variation of $\ln D$ $(\mathrm{cm}^2/\mathrm{s})$ ***as a function of*** $1000/T$ ***for FeSi at*** $P = 0$ GPa***, obtained from SMM calculations and compared with previous studies of Iijima et al. (1988) [37], Lubbehusen and Mehrer (1990) [38], and Zhang (2014) [39]***

Table 6. $Q(P, c_{\mathrm{Si}})$ ***and*** $D_0(P, c_{\mathrm{Si}})$ ***for Fe, FeSi at*** $T = 1000$ K ***calculated by SMM***

P (GPa)	$c_{\mathrm{Si}} = 0$		$c_{\mathrm{Si}} = 2\%$		$c_{\mathrm{Si}} = 4\%$	
	Q (kcal/mol)	$10^{19}D$ (cm^2/s)	Q (kcal/mol)	$10^{25}D$ (cm^2/s)	Q (kcal/mol)	$10^{31}D$ (cm^2/s)
0	56.80	870.7	67.79	2912	80.15	2666
2	56.83	165.8	67.88	505.3	80.33	419.1
4	56.87	33.59	67.99	95.71	80.53	74.17
6	56.92	7.180	68.10	19.58	80.72	14.56
8	56.97	1.611	68.22	4.286	80.91	3.126
10	57.03	0.3774	68.33	0.9950	81.09	0.7249

Table 6 illustrates how pressure (P) and silicon content influence both the diffusion coefficient (D) and activation energy (Q) in Fe and FeSi systems at 1000 K.

These findings represent the outcome of numerical calculations, along with a detailed analysis and assessment of diffusion behavior in Fe metal and the FeSi alloy.

3. Conclusions

Based on the numerical analysis of diffusion-related parameters in this paper, Fe and FeSi systems were investigated to identify four key trends. First, as temperature rises, an upward trend is observed in the pre-exponential factor, diffusion coefficient, and activation energy. Significant increases in the diffusion coefficient are primarily observed under high-temperature conditions, whereas it remains very small at lower temperatures. Second, both the pre-exponential factor and diffusion coefficient exhibit decreasing behavior under elevated pressure or applied strain (or stress). Third, the incorporation of interstitial silicon atoms results in lower values of both the pre-exponential factor and diffusion coefficient, accompanied by an increase in activation energy. Finally, plastic deformation plays a role in further reducing the pre-exponential factor and diffusion coefficient. These simulation outcomes correspond well with existing experimental data and theoretical estimates related to Fe. Meanwhile, the data for FeSi are novel and could be useful for guiding upcoming experimental work and predictive modeling.

REFERENCES

[1] Danilchenko VE, Mazanko VF, Filatov AV & Iakovlev VE, (2015). The effect of cyclic martensitic transformations on diffusion of cobalt atoms in Fe 18 wt.% Mn 2 wt.% Si alloy. *Nanoscale Research Letters*, 10, 178.

[2] Bevz VP, Bondar VI & Danilchenko VE, (2008). Diffusion regularities of carbon atoms in iron phase hardened alloy. *Metallofizika i Noveishie Tekhnologii*, 30(10), 1307-1314.

[3] Brick VB, Kumok LM, Nikolin BI & Falchenko VM, (1981). Effect of phase transformations on the diffusion mobility of atoms in iron and cobalt alloys. *Metally*, 4, 131-135.

[4] Brick VB, (1985). *Diffusion and phase transformations in metals and alloys*. Kiev: Naukova Dumka.

[5] Crank J, (1980). *The mathematics of diffusion* (2nd ed.). Oxford University Press.

[6] Mironov VM, Mironova TF, Koval YN, Gertsriken DS & Alekseeva VV, (2006). Diffusion processes in metals and alloys under martensitic transformations. *Vestnik Samara State University*, 3, 34.

[7] Aziz MJ, (1997). Thermodynamics of diffusion under pressure and stress: Relation to point defect mechanisms. *Applied Physics Letters*, 70(21), 2810-2812.

[8] Vu VH, Do DT & Nguyen TH, (2007). Effect of stress on defect diffusion in metals. *HNUE Journal of Science: Natural Science*, 52(1), 13-18.

[9] Nguyen HT & Vu VH, (1988). Investigation of the thermodynamic properties of anharmonic crystals by the momentum method (I): General results for FCC crystals. *Physica Status Solidi (b)*, 149, 511

[10] Nguyen HT & Vu VH, (1990). Investigation of the thermodynamic properties of anharmonic crystals by the momentum method (III): Thermodynamic properties of the crystals at various pressures. *Physica Status Solidi (b)*, 162, 371.

[11] Hoang VT & Vu VH, (1999). Influence of anharmonicity on the diffusion of vacancies by the moment method. In *Proceedings of the 3rd International Workshop on Materials (IWOMS 99)*, Hanoi, November 2-4, 939-942.
[12] Vu VH, Hoang VT & Do DT, (1999). Study of self-diffusion in alloys by statistical moment method: Anharmonicity effects. *Communications in Physics*, 9(4), 232-241.
[13] Masuda JK, Vu VH & Hoang VT, (1999). Self diffusion theory of vacancies in anharmonic crystals. *Proceedings of the NCST of Vietnam*, 11(2), 39-44.
[14] Vu VH, Hoang VT & Masuda JK, (2000). Study of self-diffusion in metals by statistical moment method: Anharmonicity effects. *Journal of the Physical Society of Japan*, 69(8), 2691-2699.
[15] Vu VH, Lee J, Masuda JK & Phan TTH, (2006). Study of self-diffusion in silicon at high pressure. *Journal of the Physical Society of Japan*, 75(2), 024601.
[16] Hoang VT, (2000). *Diffusion theory of metals and alloys* (PhD Thesis). Hanoi National University of Education.
[17] Nguyen QH, Dinh QV, Le HV & Nguyen VP, (2016). Study on diffusion theory of interstitial alloy AB with BCC structure. *HNUE Journal of Science: Natural Science*, 61(4), 3-9.
[18] Nguyen QH, Bui DT, Dinh QV & Le HV, (2016). Diffusion of interstitial atoms in interstitial alloys FeSi and FeH with BCC structure under pressure. *Scientific Journal of Hanoi Metropolitan University*, 61(8), 48-56.
[19] Nguyen QH, Nguyen DH & Nguyen HN, (2020). Study on the diffusion theory of BCC substitutional alloy AB with interstitial atom C. *HNUE Journal of Science: Natural Science*, 65(3), 31-38.
[20] Nguyen QH, Phan TTL, Nguyen TV & Nguyen NL, (2020). The diffusion in FCC binary interstitial alloy. *HNUE Journal of Science: Natural Science*, 65(10), 18-23.
[21] Goldschmidt HJ, (1967). *Interstitial Alloys*. London: Butterworth.
[22] Shibazaki Y, Nishida K, Higo Y, Igarashi M, Tahara M, Sakamaki T & Ohtani E, (2016). Compressional and shear wave velocities for polycrystalline BCC Fe up to 6.3 GPa and 800 K. *American Mineralogist*, 101(5), 1150-1160.
[23] TakeuchiS, (1969). Solid-solution strengthening in single crystals of iron alloys. *Journal of the Physical Society of Japan*, 27, 929-940
[24] Melnykov M & Davidchack RI, (2018). Characterization of melting properties of several Fe C model potentials. *Computational Materials Science*, 144, 273-279.
[25] Lau TT, Frst CJ, Lin X, Gale JD, Yip S & Van Vliet KJ, (2007). Many-body potential for point defect clusters in Fe C alloys. *Physical Review Letters*, 98(21), 215501.
[26] Liyanage LS, Kim SG, Houze J, Kim S, Tschopp MA, Baskes MI & Horstemeyer MF, (2014). Structural, elastic and thermal properties of cementite (Fe_4C) calculated using a modified embedded atom method. *Physical Review B*, 89, 094102.
[27] Nguyen QH & et al., (2020). On the melting of defective FCC interstitial alloy γ-FeC under pressure up to 100 GPa. *Journal of Electronic Materials*, 49, 910-916.
[28] Ppin CM, Dewaele A, Geneste G, Loubeyre P & Mezouar M, (2014). New iron

hydrides under high pressure. *Physical Review Letters*, 113(26), 265504.
[29] Terasaki H, Ohtani E, Sakai T, Kamada S, Asanuma H, Shibazaki Y & Funakoshi KI, (2012). Stability of FeNi hydride after reaction between Fe-Ni alloy and δ AlOOH up to 1.2 Mbar. *Physics of the Earth and Planetary Interiors*, 194-195, 18-24
[30] Psiachos D, Hammerschmidt T & Drautz R, (2011). Ab initio study of the modification of elastic properties of α iron by hydrostatic strain and hydrogen interstitials. *Acta Materialia*, 59(11), 4255-4263.
[31] Lee BJ & Jang JW, (2007). A modified embedded-atom method interatomic potential for the FeH system. *Acta Materialia*, 55, 6779-6788
[32] Odkhuu D, Yun WS & Hong SC, (2012). Electronic origin of the negligible magnetostriction of an electric steel $Fe_{1-x}Si_x$ alloy: A density-functional study. *Journal of Applied Physics*, 111(6), 063911
[33] Zhang J, Su C & Liu Y, (2020). First-principles study of bcc Fe-Cr-Si binary and ternary random alloys from special quasi-random structure. *Physica B: Condensed Matter*, 586, 412085.
[34] Kummerle EA, Badura K, Sepiol B, Mehrer H & Schaefer HE, (1995). Thermal formation of vacancies in Fe_3Si. *Physical Review B*, 52, R6947-R6950
[35] Zhao KM, Jiang G & Wang L, (2011). Electronic and thermodynamic properties of B2-FeSi from first-principles. *Physica B: Condensed Matter*, 406(3), 363-367
[36] Guo Z, Yuan W, Sun Y & Cai Z, (2000). Thermodynamic assessment of the Si-Ta and Si-W systems. *Journal of Phase Equilibria and Diffusion*, 30(5), 564-570.
[37] Nguyen QH, Nguyen DH, Nguyen TD & Cao VL, (2021). Study on the melting temperature, jumps of volume, enthalpy and entropy at melting point, and Debye temperature for the BCC defective and perfect interstitial alloy WSi under pressure. *Journal of Composites Science*, 5(6), 153
[38] Aziz MJ, (2001). Stress effects on defects and dopant diffusion in Si. *Materials Science in Semiconductor Processing*, 4(5), 397-403.
[39] Lazarus D, (1983). *Diffusion in Metals and Alloys*, in Kedves F.J. & Beke P.L. (Eds.).
[40] Iijima Y, Kimura K & Hirano K, (1988). Self-diffusion and isotope effect in α iron. *Acta Metallurgica,* 36(12), 2811-2820.
[41] Lubbehusen M & Mehrer H, (1990). Self-diffusion in α-iron: The influence of dislocations and the effect of the magnetic phase transition. *Acta Metallurgica et Materialia*, 38(2), 283-292.
[42] Zhang B, (2014). Calculation of self diffusion coefficients in iron. *AIP Advances*, 4, 017128.
[43] Magomedov MN, (1987). Calculation of temperature Debye and parameter Gruneisen. *Zhurnal Fizicheskoi Khimii*, 61(4), 1003-1009.
[44] Magomedov MN, (2011). Activated-process parameters for diamond, silicon and germanium crystals. *Russian Microelectronics*, 40(8), 567-573